ARTICLE
Journal of Cellular Biochemistry 113:1034–1043 (2012)

Journal of Cellular Biochemistry

Effects of Indoxyl Sulfate on Adherens Junctions of Endothelial Cells and the Underlying Signaling Mechanism

Yu-Sen Peng,[1,2] Yen-Tung Lin,[1] Ying Chen,[3] Kuan-Yu Hung,[4] and Seu-Mei Wang[1*]

[1]*Department of Anatomy and Cell Biology, College of Medicine, National Taiwan University, Taipei, Taiwan*
[2]*Division of Nephrology, Department of Internal Medicine, Far Eastern Memorial Hospital, New Taipei City, Taiwan*
[3]*Department and Graduate Institute of Biology and Anatomy, National Defense Medical Center, Taipei, Taiwan*
[4]*Division of Nephrology, Department of Internal Medicine, National Taiwan University Hospital, Taipei, Taiwan*

ABSTRACT

Uremic patients have a much higher risk of cardiovascular diseases and death. Uremic toxins are probably involved in the development of vascular endothelial dysfunction. Indoxyl sulfate (IS) is a uremic toxin that accumulates with deterioration of renal function. This study explored the effects of IS on the adherens junctions of vascular endothelial cells and revealed the underlying mechanism. Bovine pulmonary artery endothelial cells (BPAECs) were treated with IS, and the distribution of vascular endothelial cadherin (VE-cadherin), p120-catenin, β-catenin, and stress fibers was examined by immunofluorescence. IS treatment resulted in disruption of intercellular contacts between BPAECs with prominent parallel-oriented intracellular stress fiber formation. Intracellular free radical levels which measured by flow cytometry increased after IS treatment. The antioxidant, MnTMPyP, and an ERK pathway inhibitor, U0126, both significantly prevented IS-induced disruption of intercellular contacts. Western blotting analyses demonstrated that IS-induced phosphorylation of myosin light chain kinase (MLCK) and myosin light chains (MLC) as well as activation of extracellular-signal-regulated protein kinase (ERK1/ERK2). Pretreatment with MnTMPyP prevented ERK1/2 phosphorylation. U0126 prevented the IS-induced MLCK and MLC phosphorylation. MEK-ERK acted as the upstream regulator of the MLCK-MLC pathway. These findings suggest that the superoxide anion-MEK-ERK-MLCK-MLC signaling mediates IS-induced junctional dispersal of BPAECs. J. Cell. Biochem. 113: 1034–1043, 2012.

KEY WORDS: INDOXYL SULFATE; FREE RADICALS; ENDOTHELIAL CELLS; ADHERENS JUNCTION; STRESS FIBER

Accompanying the loss of kidney function, many uremic solutes accumulate and induce adverse biologic impacts. Indoxyl sulfate (IS) is a uremic toxin that is generated from the metabolism of tryptophan. Dietary tryptophan is converted into indole by intestinal bacteria. After intestinal absorption, indole is metabolized to IS in the liver. IS is eliminated by the kidney through proximal tubular secretion and accumulates in the blood of patients with chronic kidney disease (CKD) [Niwa et al., 1988; Atoh et al., 2009]. Furthermore, because of its high-binding affinity with serum albumin, IS cannot be efficiently removed by hemodialysis [Niwa et al., 1988].

The adverse biologic effect of IS was first demonstrated by its accelerating effects on glomerular sclerosis [Niwa and Ise, 1994]. IS stimulates the transcription of genes related to renal fibrosis, such as transforming growth factor-β1, tissue inhibitor of metalloproteinase-1, and pro-α1 collagen [Miyazaki et al., 1997]. IS has also been reported to stimulate the formation of free radicals, plasminogen activator inhibitor 1, and activated nuclear factor-κB in renal tubular cells [Motojima et al., 2003].

Compared to the general population, patients with CKD have a much higher risk of cardiovascular disease and death [Vanholder et al., 2005]. The role of uremic toxins in the pathogenesis of CKD-related cardiovascular risk deserves to be explored.

The association of IS and vascular injury has been studied in many cellular experiments. IS directly stimulates rat vascular smooth muscular cell proliferation in a concentration-dependent manner [Yamamoto et al., 2006]. In endothelial cells, it induces the formation of reactive oxygen species (ROS) via increased NADPH oxidase activity [Dou et al., 2007]. IS has also been reported to stimulate the release of endothelial micro particles [Faure et al., 2006] and impair endothelial healing ability [Dou et al., 2004]. Furthermore, recent clinical studies reported that higher serum

Grant sponsor: Nation Science Council; Grant number: NSC 97-2320-B002-051-MY3; Grant sponsor: Far Eastern Memorial Hospital; Grant number: FEMH-99-C-015.
*Correspondence to: Seu-Mei Wang, Department of Anatomy and Cell Biology, College of Medicine, National Taiwan University, 1-1 Jen-Ai Road, Taipei 10051, Taiwan. E-mail: smwang@ntu.edu.tw
Received 17 January 2011; Accepted 25 October 2011 • DOI 10.1002/jcb.23435 • © 2011 Wiley Periodicals, Inc.
Published online 28 December 2011 in Wiley Online Library (wileyonlinelibrary.com).

concentration of IS was a risk factor for atherosclerosis in CKD patients [Taki et al., 2007; Barreto et al., 2009]. These findings suggest that IS plays a role in endothelial dysfunction in CKD patients.

The barrier function is one of important functions of vascular endothelium. Uremic plasma had been found to induce a breakdown of the endothelial barrier function for macromolecules in an animal study [Harper et al., 2002]. This suggests that uremic toxins play a role in the endothelial barrier dysfunction. Barrier dysfunction results from the formation of gaps between adjacent cells as a consequence of loss of intercellular junctions. The maintenance of intact endothelial barrier function depends on two groups of protein molecules.

First one is an intact intercellular junction complex. Adherens junctions form connections between adjacent cells through the homophilic binding of the extracellular domain of vascular endothelial cadherin (VE-cadherin), a transmembrane vascular-specific cadherin. Furthermore, intact adherens junctions are essential for maintenance of intercellular tight junctions [Dejana et al., 2008].

The other is the adequate actin–myosin cytoskeleton organization. Within the cell, VE-cadherin is linked to the actin–myosin cytoskeleton via β-catenin and α/γ-catenin. The cytoskeleton plays a central role in the regulation of endothelial permeability and cell migration by controlling cell shape [Lee et al., 2001; Deguchi and Sato, 2009]. Activation of the endothelial contractile machinery and generation of contractile forces by endothelial cells can cause adjacent cells to retract from each other. It has been demonstrated that an increase in non-muscle myosin II light chain (MLC) phosphorylation is associated with cellular contraction [Wysolmerski and Lagunoff, 1990]. Endothelial cell myosin II activation is linked by signal transduction pathways composed of intracellular kinases and phosphatases. Both Ca^{2+}-dependent and Ca^{2+}-independent pathways activate myosin II motor activity [Fukata et al., 2001; Somlyo and Somlyo, 2003]. Ca^{2+}-dependent cell contraction is mediated by Ca^{2+}/calmodulin-dependent protein kinase II (CaMK II) and myosin light chain kinase (MLCK), and MLCK catalyzes the phosphorylation of MLC at Ser^{19} and Thr^{18} [Goeckeler and Wysolmerski, 1995], which leads to myosin II filament formation, the interaction of myosin II with F-actin, and increased myosin II ATPase activity. Another cascade to enhance MLCK activity is mitogen-activated protein kinase (MAPK) pathway [Klemke et al., 1997]. The extracellular-signal-regulated protein kinase (ERK1/ERK2) influences the cells' motility machinery by phosphorylating and, thereby, enhancing MLCK activity leading to phosphorylation of MLC. The cells become elongated and migratory [Lee et al., 1996] and show cellular junction disruption and intercellular gap formation [McKenzie and Ridley, 2007].

To our knowledge, no study has addressed the effects of IS on vascular endothelial permeability, the cell junction, and the cytoskeleton. A previous study has reported that IS blunts endothelial healing ability and proliferation [Dou et al., 2004]. The exact underlying mechanism of this blunted endothelial healing ability has not been clarified. We postulated that IS has an impact on the organization of the endothelial cytoskeleton system. The objects of this study were to examine the effects of IS on vascular endothelial barrier function and to explore changes in the adherens junction and cytoskeleton and the underlying mechanisms.

MATERIALS AND METHODS

CELL CULTURE

Bovine pulmonary artery endothelial cells (BPAECs) were obtained from the American Type Tissue Culture Collection (Manassas, VA, culture line-CCL 209) and used at passages 4–8. Cells were maintained in complete culture medium consisting of Dulbecco's modified Eagle's medium (DMEM) containing 10% bovine serum, endothelial cell growth supplement (17 μg/ml, H-neurext; Upstate Biotechnology Inc., Charlottesville, VA), and 100 U/ml of penicillin/streptomycin (Gibco-BRL) at 37°C in a humidified atmosphere of 95% air and 5% CO_2.

REAGENTS

Purified IS powder, 4 kDa fluorescein isothiocyanate-dextran (FITC-dextran 3000), and 3-(4,5-dimethylthiazol-2-yl)-2,5-diphenyltetrazolium bromide (MTT) were obtained from Sigma–Aldrich (St. Louis, MO). Rhodamine phalloidin was purchased from Cytoskeleton Inc (Denver, CO). The extracellular signal-related kinase (ERK) inhibitor U0126 was purchased from Biolmol Research Laboratories (Plymouth Meeting, PA) and was used at a concentration of 10 μM. Manganese (III) tetrakis (1-methyl-4-pyridyl) porphyrin pentachloride (MnTMPyP) was purchased from Cayman Chemical (Ann Arbor, MI). The primary mouse monoclonal antibodies used were anti-β-catenin, anti-p120 catenin (BD Bioscience, San Jose, CA), and anti-phospho-ERK1/2 (Santa Cruz Biotechnology Inc., Santa Cruz, CA). The primary rabbit polyclonal antibodies were anti-$pSer^{19}$-MLC (Sigma–Aldrich), anti- $pSer^{1760}$-MLCK (Invitrogen, Camarillo, CA), anti-VE-cadherin (Alexis Biochemicals, San Diego, CA), and anti-phospho-MEK1/2 (Cell Signaling, Technology, Inc., Danvers, MA).

For Western blots, all primary antibodies were used at a 1:500 dilution and the secondary antibodies were alkaline phosphatase-conjugated anti-rabbit or anti-mouse IgG antibodies (1:7,500 dilutions, Promega Corp., Madison, WI). The antibodies for internal standards includes rabbit ERK (Santa Cruz), rabbit anti-MEK (Epitomics), rabbit anti-MLCK (Epitomics), and rabbit anti-MLC (Epitomics, Cell Signaling). For immunofluorescence studies, the above primary rabbit anti-VE-cadherin and mouse anti-β-catenin and anti-p120 catenin antibodies were used and the secondary antibodies were Texas red-conjugated goat anti-rabbit IgG antibodies (Jackson Immuno Research, West Grove, PA) and FITC-conjugated goat anti-mouse IgG antibodies (Sigma–Aldrich).

MTT ASSAY

The MTT assay was used to examine whether cell viability was affected by IS. Briefly, BPAECs (4×10^3 cells/well) were suspended in 200 μl of complete culture medium and plated on 24-well cell culture plates. After 24 h, the cells were treated with complete culture medium containing 50–250 μg/ml of IS for 24 h, then were incubated for 4 h with MTT solution [5 mg/ml in phosphate-buffered saline (PBS) diluted tenfold in serum-free DMEM] and the optical

density measured at 590 nm using an ELISA reader (Molecular Devices, San Francisco, CA).

IMMUNOFLUORESCENCE

After various treatments, BPAECs were fixed for 10 min at room temperature in 100% acetone and non-specific binding blocked by incubation with 5% non-fat milk in PBS for 30 min. The cells were then incubated for 1 h at 37°C with the primary antibodies, washed with PBS (3 × 5 min), and incubated for 1 h at 37°C with FITC-conjugated goat anti-rabbit IgG or FITC-conjugated goat anti-mouse IgG antibodies. Images were taken on a Zeiss Axiophot epifluorescence microscope (Carl Zeiss, Oberkochen, Germany) equipped with a Nikon D1X digital camera (Nikon, Tokyo, Japan).

ENDOTHELIAL PERMEABILITY ASSAY

The permeability assay was performed according to the instruction of Chemicon International for in vitro permeability assay. 10^5 cells (150 μl) was seeded in the pre-wet upper well of a Transwell apparatus with a pore size of 3 μm (Costar, Acton, MA), and 500 μl of culture medium was added to the lower chamber. Cells were grown for 3 days to reach confluence examined by Coomassie blue staining. After wash with 10 mM HEPES buffer (pH 7.4), 150 μl of FITC-dextran 3000 (10 μg/ml) was added to the upper chamber and 0.5 ml of HEPES buffer to the lower chamber, and 2 h later, 100 μl from the lower chamber was collected and analyzed by the Paradigm™ detection platform (Beckman, Coulter) using excitation/emission wavelengths of 490/520 nm.

WESTERN BLOT ANALYSIS

To prepare whole cell lysates, BPAECs were scraped off the culture dish in lysis buffer (0.15% Triton X-100, 10 mM EGTA, 2 mM $MgCl_2$, 60 mM PIPES, 25 mM HEPES, pH 6.9) and sonicated for twenty 10-s pulses, then the protein concentration of the lysate was determined using a protein assay kit (Bio-Rad, Hercules, CA). Fifty micrograms of protein was applied to each lane of a 10% polyacrylamide–SDS gel, subjected to electrophoresis, and transferred to nitrocellulose paper (Schleicher and Schuell BioSciences, Boston, MA). Membrane strips were blocked for 1 h at room temperature with 5% non-fat milk in Tris-buffered saline (TBS; 150 mM NaCl, 50 mM Tris base, pH 8.2) containing 0.1% Tween 20, then incubated overnight at 4°C with primary antibodies. They were then incubated for 1 h at room temperature with alkaline phosphatase-conjugated secondary antibodies and positive bands visualized using nitro blue tetrazolium and 5-bromo-4-chloro-3-indolyl phosphate as chromogen (3.3 mg/ml of nitroblue tetrazolium and 1.65 mg/ml of 5-bromo-4-chloro-3-indolyl phosphate in 100 mM NaCl, 5 mM $MgCl_2$, 100 mM Tris, pH 9.5). Densitometry was performed using Gel Pro 3.1 (Media Cybernetics, Silver Spring, MD). All experiments were performed three times and the values are expressed as the mean ± SD.

FLOW CYTOMETRY MEASUREMENTS OF INTRACELLULAR REACTIVE OXYGEN SPECIES

Intracellular levels of superoxide anions in BPAECs were assessed using dihydroethidium (DHE) (Molecular Probe Inc.) and MitoSox (Molecular Probe Inc.). BPAECs were loaded with 10 μM DHE or 5 μM MitoSox™ in complete culture media for 10 and 15 min, respectively, at 37°C in the dark, then 1×10^6 cells were washed once with PBS, trypsinized, collected, and analyzed immediately. All analyses were performed using a BD FACSCalibur flow cytometer (Beckton Dickinson Immunocytometry Systems, San Jose, CA) equipped with a 15 mW argon-ion laser tuned at 488 nm.

STATISTICS

Results are presented as the mean ± SD for three replicate experiments. Statistical differences between means were evaluated using Student's *t*-test. Differences were considered significant when $P < 0.05$.

RESULTS

EFFECT OF IS ON ENDOTHELIAL CELL VIABILITY

Cytotoxicity of IS for BPAECs was evaluated using the MTT assay. As shown in Figure 1, treatment for 24 h with 50, 100, 200, or 250 μg/ml of IS had no significant effect on cell viability.

IS DISRUPTS CONTINUOUS INTERCELLULAR CONTACTS BETWEEN ENDOTHELIAL CELLS

The effects of IS on adherens junctions were examined in an immunofluorescence study. In BPAECs without IS treatment, continuous linear staining for p120-catenin (Fig. 2A), VE-cadherin (Fig. 2D), and β-catenin (Fig. 2G) was seen at cell–cell contacts, whereas, after 24 h treatment with 100 μg/ml of IS, intercellular gap formations and discontinuous staining was detected for p120-catenin (Fig. 2B), VE-cadherin (Fig. 2E), and β-catenin (Fig. 2H). In cells treated with 250 μg/ml of IS for 24 h, the intercellular gaps were larger, and staining for p120-catenin (Fig. 2C), VE-cadherin (Fig. 2F), and β-catenin (Fig. 2I) decreased further. These results revealed a dose-dependent decrease in cell–cell contact areas and junctional dispersal induced by IS treatment.

About 40% of the cells exhibited spitting of cell junction. Using FITC-dextran permeability assay, we detected 17% increase in endothelial permeability (Fig. 3).

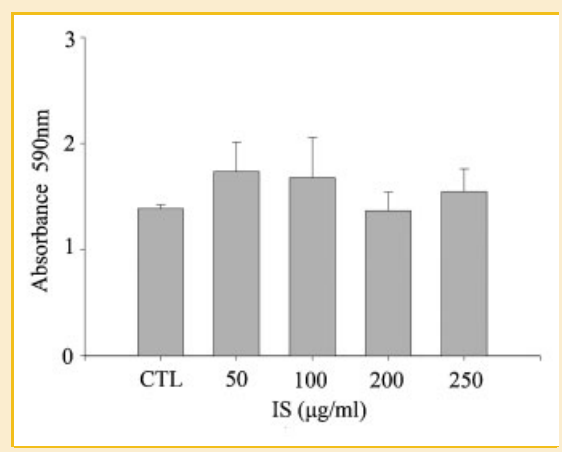

Fig. 1. Effect of IS on the cytotoxicity of BPAECs. The cells were incubated for 24 h in control medium (CTL) or medium containing 50–250 μg/ml of IS, then cell viability was determined using the MTT assay (N = 3).

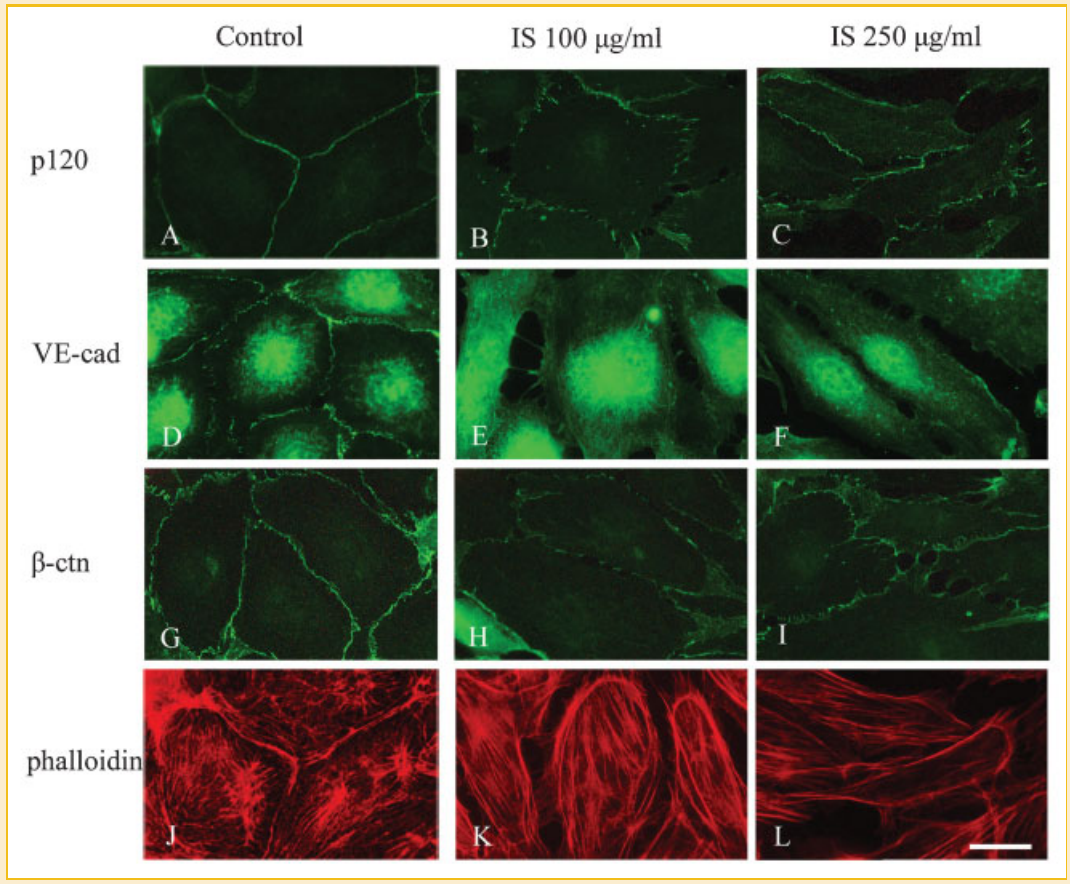

Fig. 2. IS induces adherens junction disassembly, stress fiber reorganization, and intercellular gap formation in BPAECs. BPAECs were treated for 24 h with control medium (A, D, G, and J) or medium containing 100 μg/ml of IS (B, E, H, and K) or 250 μg/ml of IS (C, F, I, and L), then immunostained for p120-catenin (p120) (A–C), VE-cadherin (VE-cad) (D–F), β-catenin (β-ctn) (G–I), or phalloidin (J–L). Bar = 20 μm. [Color figure can be seen in the online version of this article, available at http://wileyonlinelibrary.com/journal/jcb]

THE IS-INDUCED JUNCTIONAL DISRUPTION IS MEDIATED BY CYTOSKELETON REORGANIZATION AND CELL CONTRACTION

As shown in Figure 4C-a, control BPAECs showed a cobble stone-like shape, while, in the presence of IS, the cells became elongated and even showed a fibroblast-like appearance (Fig. 4C-c). Because the cytoskeletal architecture is the main determinant of cell morphology, we examined the effects of IS on the actin cytoskeleton. Control BPAECs showed randomized arrays of staining of the actin cytoskeleton (Fig. 4C-b), while after IS treatment for 24 h, prominent parallel-oriented stress fiber formation was seen (Fig. 4C-d).

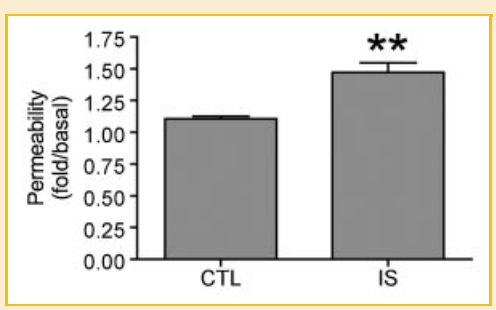

Fig. 3. IS treatment induced paracellular FITC-dextran permeability. The data represent the mean ± SD from four independent experiments. $^{**}P < 0.01$, compared to the control group.

INVOLVEMENT OF SUPEROXIDE IN IS-INDUCED ENDOTHELIAL JUNCTIONAL DISRUPTION

We next examined the role of ROS in the IS-induced endothelial junctional disruption in BPAECs. We measured production of superoxide anions and hydrogen peroxide by cells after IS treatment using DHE or dichlorofluorescein diacetate, respectively, and found that only superoxide anions increased (data not shown). Previous studies also supported that IS induced superoxide production [Owada et al., 2008]. We therefore focused on superoxide production by using the superoxide anion indicator DHE and MitoSox^{TM} in flow cytometry. After treatment with 250 μg/ml of IS for 10 and 15 min, the amount of superoxide anions increased (Fig. 4A,B). For confirmation of the role of superoxide anion, the cell-permeable specific superoxide dismutase mimetic, MnTMPyP, was used to test the protective effect from IS-induced junction disruption. Figure 4C (e-f) illustrates that MnTMPyP significantly inhibited the IS-induced cellular junction disruption, intercellular gap formation, stress fiber formation, and cell shape change, suggesting that the IS-induced

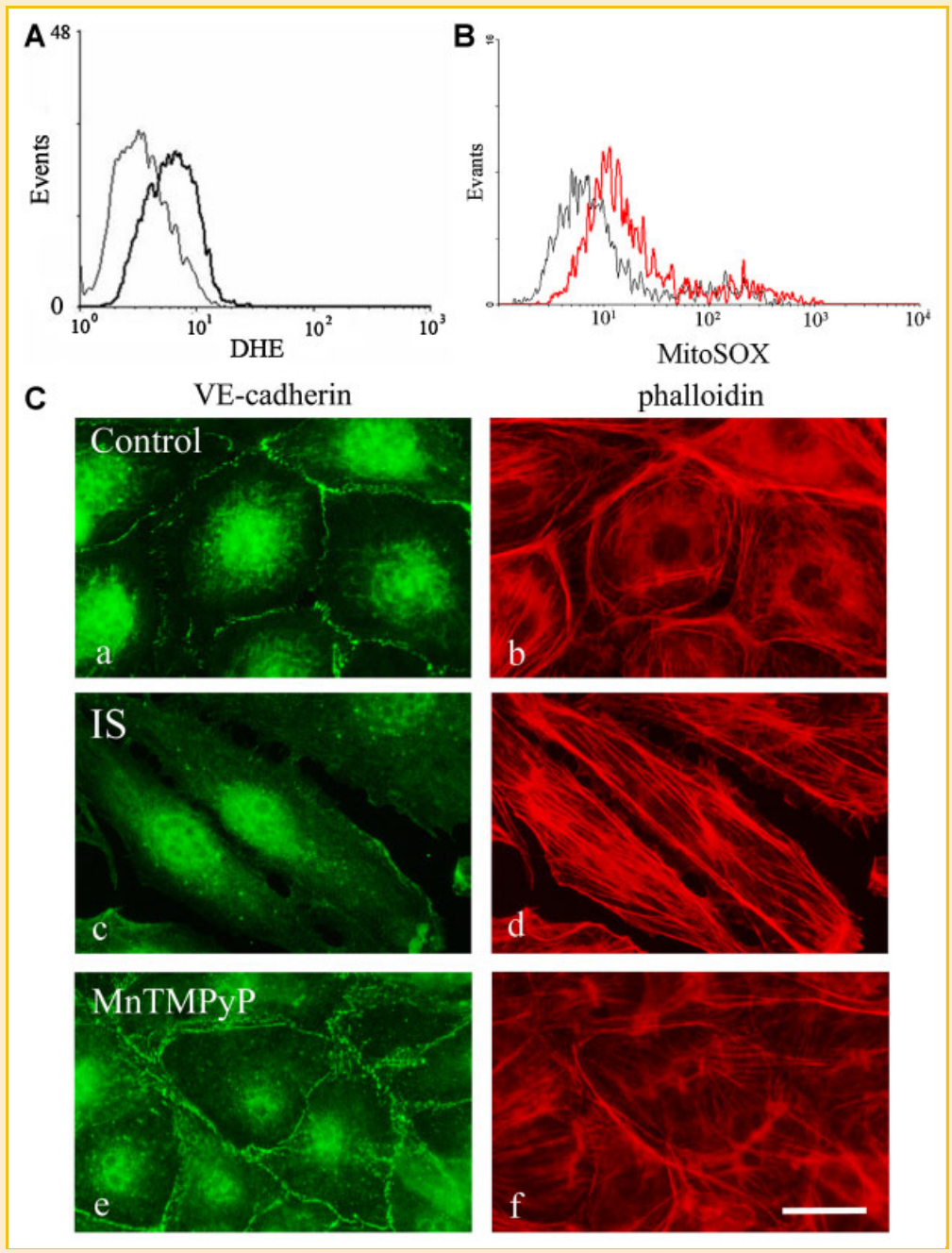

Fig. 4. Effect of IS treatment on intracellular superoxide anion generation. BPAECs were treated with 250 μg/ml of IS for 10 min, then superoxide anion generation was examined using DHE (A) and MitoSox™ (B) and flow cytometry. The results are representative of those obtained in six experiments. The light trace is without IS treatment and the dark trace with IS treatment. The horizontal axis represents the geometric red fluorescence intensity and the vertical axis the cell number. C: MnTMPyP prevents the IS-induced decrease in VE-cadherin at adherens junctions and stress fiber formation. BPAECs were incubated for 24 h with control medium (a, b), 250 μg/ml of IS (c, d), or IS plus 6 μM MnTMPyP (e, f) and processed for immunofluorescence staining for VE-cadherin (a, c, and e) or phalloidin (b, d, and f). Bar = 20 μm. [Color figure can be seen in the online version of this article, available at http://wileyonlinelibrary.com/journal/jcb]

junctional disruption in BPAECs is mediated by the generation of superoxide anions.

THE ERK PATHWAY IS ACTIVATED AFTER IS TREATMENT AND U0126 PREVENTS IS-INDUCED ENDOTHELIAL BARRIER DISRUPTION

Because the ERK pathway could phosphorylate and activate MLCK [Klemke et al., 1997], we explored the impact of IS on the ERK pathway. Inhibition tests with the ERK pathway inhibitor U0126 were done. In the immunofluorescence studies, control BPAECs showed a cobble-stone-like shape and intercellular junctions were continuous (Fig. 5A,B). After 24 h treatment with 250 μg/ml of IS, intercellular gap formations, discontinuous staining for p120-catenin, parallel-oriented stress fiber formation, and cell elongation were noted (Fig. 5C,D). Pretreatment with 10 μM of U0126 before IS

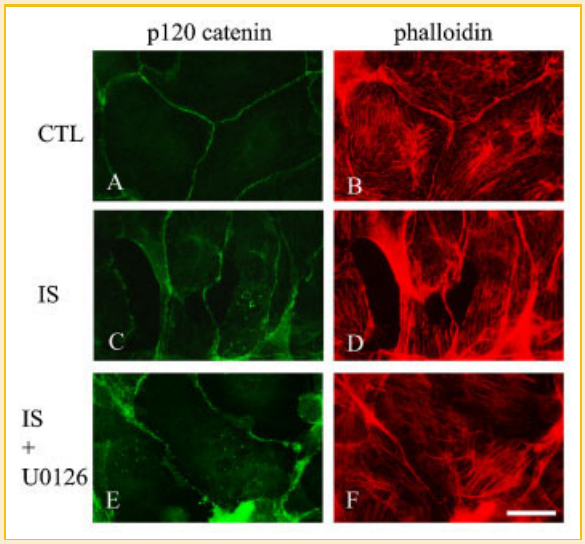

Fig. 5. U0126 prevents IS-induced adherens junction disassembly, stress fiber reorganization, and intercellular gap formation in BPAECs. Cells were incubated with control medium for 24 h (A and B), 250 μg/ml IS (C and D) for 24 h, or 10 μM U0126 for 30 min, then 250 μg/ml IS for 24 h (E and F), then immunostained for p120-catenin (A, C, and E) or phalloidin (B, D, and F). Bar = 20 μm. [Color figure can be seen in the online version of this article, available at http://wileyonlinelibrary.com/journal/jcb]

incubation preserved the cobble-stone-like shape of BPAECs, intact intercellular junctions, and randomized arrays of staining of the actin cytoskeleton (Fig. 5E,F). These data suggest that there was ERK pathway activation after IS treatment. We further examined this possibility by Western blotting analyses. As expected, IS treatment induced MEK (Fig. 6A) and ERK1/2 (Fig. 6B) phosphorylation significantly at 15 min. We further traced the pERK proteins by the immunofluorescence study. After 24 h treatment with 250 μg/ml of IS, the pERK translocated into the nuclei from cytoplasm (Fig. 6C).

IS ACTIVATES ERK PATHWAY BY INCREASING SUPEROXIDE LEVELS

For further clarifying the relationship of increasing superoxide levels and ERK activation, we did the inhibition tests of MnTMPyP by Western analyses. Pretreatment with 6 μM MnTMPyP also significantly decreased the ERK1/2 phosphorylation by IS (Fig. 7). It suggests that IS activates ERK pathway by increasing ROS levels.

IS INDUCES MLCK/MLC PHOSPHORYLATION THROUGH ERK PATHWAY

In the above experiments, reorganization of the actin cytoskeleton was demonstrated. To explore the underlying mechanism, we assessed the effects of IS treatment on the MLC phosphorylation cascade. As shown in Figure 8A, MLCK phosphorylation increased with time of treatment (15–60 min) with 250 μg/ml of IS. Consistent with these findings, IS also caused a significant increase in phosphorylation of MLC (Fig. 8B) that reached highest level at 2 h. U0126 pretreatment prevented the IS-induced MLCK phosphorylation (Fig. 8C). According to previous analyses, we conclude that

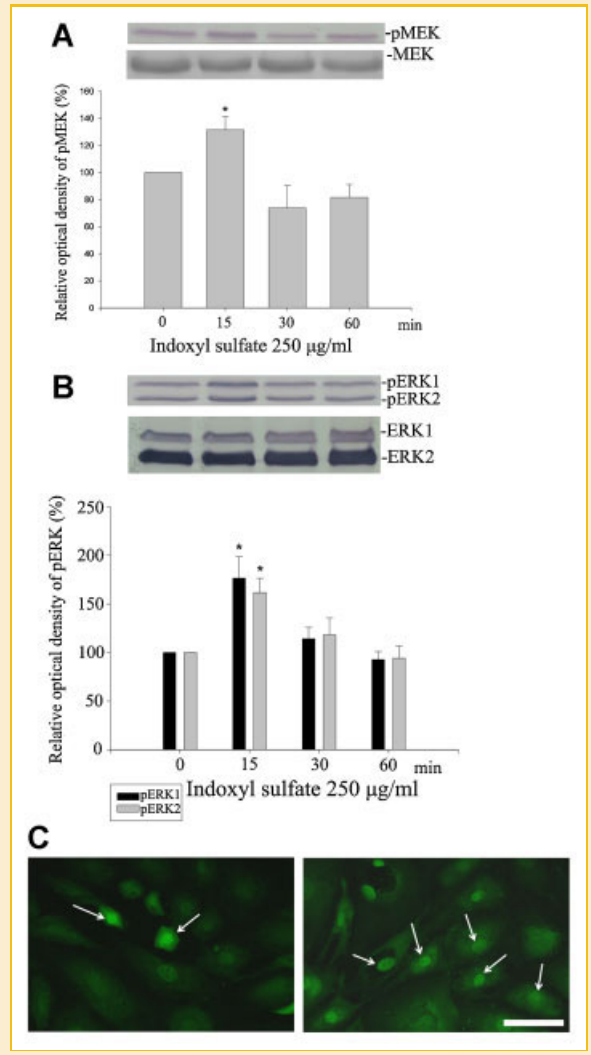

Fig. 6. IS treatment activates the MEK-ERK pathway. BPAECs were incubated for 0, 15, 30, or 60 min with 250 μg/ml IS, then cell homogenates analyzed for pMEK (A), pERK1/pERK2 (B), MEK, and ERK1/2 (loading control) (N = 3). $^{*}P < 0.05$ as compared to the 0 min value. C: BPAECs were incubated for 24 h with control medium or 250 μg/ml IS, then processed for immunostaining for pERK. It demonstrates that translocation of pERK into the nuclei by IS. [Color figure can be seen in the online version of this article, available at http://wileyonlinelibrary.com/journal/jcb]

free radicals-MEK-ERK-MLCK-MLC signaling mediates IS-induced junctional dispersal of BPAECs. Figure 9 is a schematic representation of the IS-induced signaling pathways for junctional dispersal.

DISCUSSION

In the present study, we examined the effect of IS on vascular endothelial barrier function and underlying signaling cascades. The results show that IS induces vascular endothelial cytoskeleton remodeling and cell contraction to disrupt intercellular junction. IS induces increase of superoxide anions, which induced endothelial cytoskeleton remodeling regulated by the MEK-ERK-

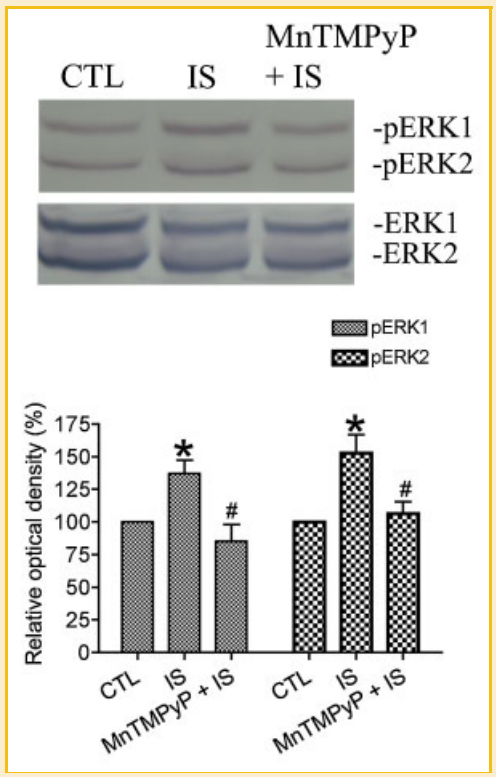

Fig. 7. Anti-oxidant MnTMPyP treatment prevents IS induced-increase of pERK. BPAECs were incubated with control media for 15 min, 250 μg/ml IS for 15 min, or pre-incubated with 6 μM MnTMPyP for 30 min, then 250 μg/ml IS for another 15 min, and then whole cell lysates were subjected to electrophoresis and immunoblotting with antibodies against ERK1/2 or pERK1/2 (N = 4). $^{*}P < 0.05$ versus the control. $\#P > 0.05$ versus the IS-groups.

MLCK-MLC pathway. MnTMPyP prevented IS-induced MEK-ERK activation and barrier dysfunction. These results indicate that intracellular redox regulation by IS plays a crucial role in superoxide-mediated activation of MAPK and barrier dysfunction in vascular endothelium.

Endothelial barrier function is an important component in the maintenance of the integrity of the vascular bed. An increased vascular permeability allows plasma components and inflammatory cells to exit the vessels. Pulmonary edema is a common complication in both acute and chronic renal failure. Its pathogenesis is multi-factorial. A previous report demonstrated an increased protein concentration in the pulmonary edema fluid of patients with renal failure [Rackow et al., 1978], suggesting that pulmonary vascular permeability is altered and explaining the occurrence of pulmonary edema in patients who do not have any other clinically features of heart failure. Furthermore, an increased vascular permeability is associated with development of atherosclerosis [Colangelo et al., 1998; Lee et al., 2008]. In animal studies, the initiating event in atherosclerosis is an elevated vascular endothelial permeability for the passage of lipid, specifically low-density lipoprotein (LDL), into the subendothelial space [Schwenke and Carew, 1989; Nielsen et al., 1992]. Atherosclerotic lesion-prone areas have also been shown to exhibit enhanced vascular permeability to albumin, LDL, and cholesterol [Fry et al., 1993].

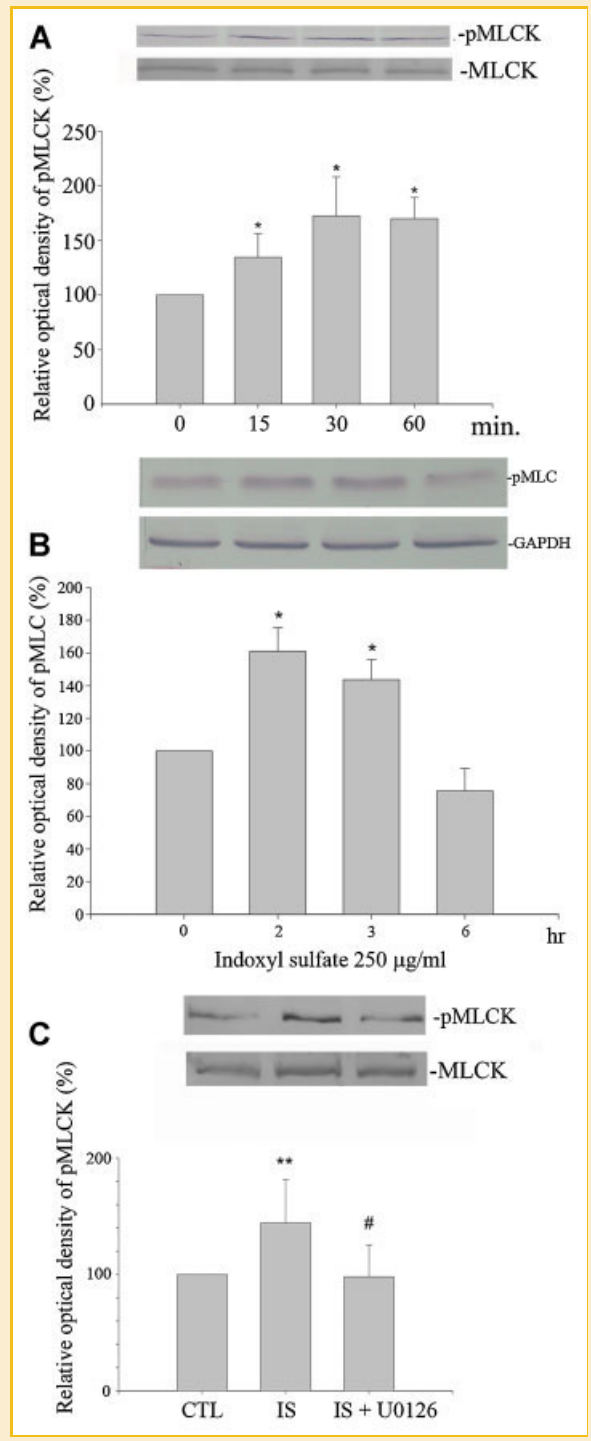

Fig. 8. IS treatment induces phosphorylation of MLCK and MLC. Pretreatment with U0126 prevents IS-induced phosphorylation of MLCK (A). BPAECs were treated with 250 μg/ml IS for 0, 15, 30, or 60 min, then whole cell homogenates analyzed for phospho-MLCK or GAPDH. (B) BPAECs were treated with 250 μg/ml IS for 0, 2, 3, 6 h, then whole cell homogenates analyzed for phospho-MLC or GAPDH (N = 3). $^{*}P < 0.05$ as compared to the 0 min value. C: BPAECs were incubated with control media for 60 min, 250 μg/ml IS for 60 min, or pre-incubated with 10 μM U0126 for 30 min, then 250 μg/ml IS for more 60 min, then whole cell lysates were subjected to electrophoresis and immunoblotting with antibodies against phospho-MLCK or GAPDH (N = 3). $^{**}P < 0.01$ versus the control groups. $\#P < 0.05$ versus the IS-group.

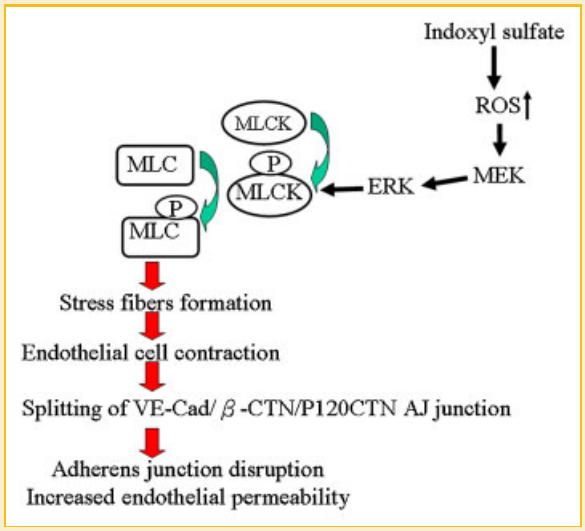

Fig. 9. Summary of major findings: IS-induced vascular endothelial barrier dysfunction by the disrupting intercellular junctions and inducing formation of intercellular gaps. ROS increase, MEK/ERK activation, MLCK/MLC phosphorylation, and cytoskeleton actin–myosin rearrangement are all involved in this cascade. [Color figure can be seen in the online version of this article, available at http://wileyonlinelibrary.com/journal/jcb]

In a human tissue study, compromised endothelial integrity was found in atheroma plaques and was associated with extensive leukocyte infiltration, intraplaque hemorrhage, and plaque instability [Sluimer et al., 2009]. Our results show that IS causes marked impairment of the vascular endothelial junction, an early pathologic change of vascular endothelial dysfunction and atherosclerosis. It might explain the extremely high prevalence of atherosclerosis in kidney failure patients. Exploring the underlying signaling mechanism is conductive to develop the therapeutic strategy of cardiovascular disease in kidney failure patients.

Previous studies reported that IS-enhanced ROS production in endothelial cells by increasing NAD(P)H oxidase activity, decreasing glutathione levels [Dou et al., 2007], and induction of NADPH oxidase 4 gene expression [Tumur and Niwa, 2009]. In fact, mitochondria are the major sources of ROS production [Rocha et al., 2010]. In this study, one indicator we used in flow cytometry was MitoSox^{TM}, a sensitive indicator of mitochondrial superoxide. Our result proves that IS induces superoxide production from mitochondria. A recent study also reported that IS increased mitochondrial superoxide production [Owada et al., 2008].

The ROS-induced barrier dysfunction has been studied in endothelial cells. Previous studies suggest that ROS-mediated permeability changes in endothelial cells involve activation of protein kinase C [Siflinger-Birnboim et al., 1992], Src kinase [Shi et al., 2000], Rho/Rho kinase pathway [Sanchez et al., 2007], and calcium influx [Zhou et al., 2009]. U0126 is a highly specific inhibitor of MEK1/2. In this study, U0126 treatment prevented IS induced cell junction disruption. This result demonstrates the role of MEK-ERK activation regulating IS-induced barrier dysfunction. MnTMPyP is a cell permeable superoxide dismutase mimetic. The MnTMPyP pretreatment blocked ERK1/2 phosphorylation and barrier dysfunction, implicating IS causes MEK-ERK activation and endothelial permeability changes via increasing superoxide anions levels. In a previous study of lung microvascular endothelial cells, H_2O_2 induced barrier dysfunction by p38 MAP kinase activation but not ERK [Usatyuk et al., 2003]. In our study, flow cytometry detected superoxide levels, but not H_2O_2, increase after IS treatment. However, we can not exclude the involvement of other types of ROS in this event.

The ERK pathway is one of the subfamily of MAPK. The ERK pathway of endothelial permeability is significantly activated by IS treatment. We demonstrated that active ERK directly promoted MLCK phosphorylation as a prior study [Klemke et al., 1997]. ERK pathway has been implicated in the migration of cancer cells, leukocytes, and smooth muscle cells. A recent study of human umbilical vein endothelial cell demonstrated that activated ERK signaling-induced endothelial hyperpermeability [Huang et al., 2004].

Although IS binds strongly to proteins in serum previous study reported that the presence of albumin at concentrations encountered in kidney failure patients did not affect the ability of IS to induce ROS production in endothelial cells [Dou et al., 2004]. Serum IS levels are up to 50-fold higher in uremic patients than in healthy subjects, the maximal IS concentration being about 240 μg/ml [Vanholder et al., 2003] which nearly the same to our test dose, 250 μg/ml. In fact, our study demonstrated the development of vascular endothelial barrier dysfunction caused by IS treatment at a dose-dependent manner. At the concentration of 100 μg/ml, IS induced obvious intercellular gap formation and cytoskeleton rearrangement in immunofluorescence study.

The main limitation of this study is that it was performed in vitro. We did not study the impact of blood flow on the effects of IS. In vivo, vascular endothelial cells are constantly exposed to shear stress as a result of blood flow, and shear stresses have been shown to affect endothelial barrier function [Karmakar, 2001; Ogunrinade et al., 2002]. Another study also reported that, after exposed to disturbed flow, discontinuous VE-cadherin staining on BPAECs and the presence of gaps in the intercellular junction were demonstrated [Miao et al., 2005]. Because shear stress by blood flow and IS exposure both induce vascular endothelial junction disruption, it is difficult to clarify the role of IS in animal study.

In summary, we have shown that IS treatment of BPAECs results in the remodeling of cytoskeleton, cell contraction, and intercellular gaps formation. IS induces increase of superoxide anions, MEK/ERK phosphorylation, and MLCK/MLC phosphorylation. Pretreatment with U0126 prevented MLCK phosphorylation and intercellular gaps formation. Increased phosphorylation of ERK and intercellular gaps formation by IS were prevented by pretreatment of cells with MnYMPyP. IS-induced endothelial cytoskeleton remodeling and intercellular gaps formation both are regulated by the superoxide anion-MEK-ERK-MLCK-MLC pathway (Fig. 9).

REFERENCES

Atoh K, Itoh H, Haneda M. 2009. Serum indoxyl sulfate levels in patients with diabetic nephropathy: Relation to renal function. Diabetes Res Clin Pract 83:220–226.

Barreto FC, Barreto DV, Liabeuf S, Meert N, Glorieux G, Temmar M, Choukroun G, Vanholder R, Massy ZA. 2009. Serum indoxyl sulfate is associated with vascular disease and mortality in chronic kidney disease patients. Clin J Am Soc Nephrol 4:1551–1558.

Colangelo S, Langille BL, Steiner G, Gotlieb AI. 1998. Alterations in endothelial F-actin microfilaments in rabbit aorta in hypercholesterolemia. Arterioscler Thromb Vasc Biol 18:52–56.

Deguchi S, Sato M. 2009. Biomechanical properties of actin stress fibers of non-motile cells. Biorheology 46:93–105.

Dejana E, Orsenigo F, Lampugnani MG. 2008. The role of adherens junctions and VE-cadherin in the control of vascular permeability. J Cell Sci 121:2115–2122.

Dou L, Bertrand E, Cerini C, Faure V, Sampol J, Vanholder R, Berland Y, Brunet P. 2004. The uremic solutes p-cresol and indoxyl sulfate inhibit endothelial proliferation and wound repair. Kidney Int 65:442–451.

Dou L, Jourde-Chiche N, Faure V, Cerini C, Berland Y, Dignat-George F, Brunet P. 2007. The uremic solute indoxyl sulfate induces oxidative stress in endothelial cells. J Thromb Haemost 5:1302–1308.

Faure V, Dou L, Sabatier F, Cerini C, Sampol J, Berland Y, Brunet P, Dignat-George F. 2006. Elevation of circulating endothelial microparticles in patients with chronic renal failure. J Thromb Haemost 4:566–573.

Fry DL, Herderick EE, Johnson DK. 1993. Local intimal-medial uptakes of 125I-albumin, 125I-LDL, and parenteral Evans blue dye protein complex along the aortas of normocholesterolemic minipigs as predictors of subsequent hypercholesterolemic atherogenesis. Arterioscler Thromb 13:1193–1204.

Fukata Y, Amano M, Kaibuchi K. 2001. Rho-Rho-kinase pathway in smooth muscle contraction and cytoskeletal reorganization of non-muscle cells. Trends Pharmacol Sci 22:32–39.

Goeckeler ZM, Wysolmerski RB. 1995. Myosin light chain kinase-regulated endothelial cell contraction: The relationship between isometric tension, actin polymerization, and myosin phosphorylation. J Cell Biol 130:613–627.

Harper SJ, Tomson CR, Bates DO. 2002. Human uremic plasma increases microvascular permeability to water and proteins in vivo. Kidney Int 61:1416–1422.

Huang C, Jacobson K, Schaller MD. 2004. MAP kinases and cell migration. J Cell Sci 117:4619–4628.

Karmakar N. 2001. Interaction of transmural pressure and shear stress in the transport of albumin across the rabbit aortic wall. Atherosclerosis 156:321–327.

Klemke RL, Cai S, Giannini AL, Gallagher PJ, de Lanerolle P, Cheresh DA. 1997. Regulation of cell motility by mitogen-activated protein kinase. J Cell Biol 137:481–492.

Lee TY, Rosenthal A, Gotlieb AI. 1996. Transition of aortic endothelial cells from resting to migrating cells is associated with three sequential patterns of microfilament organization. J Vasc Res 33:13–24.

Lee TY, Noria S, Lee J, Gotlieb AI. 2001. Endothelial integrity and repair. Adv Exp Med Biol 498:65–74.

Lee K, Saidel GM, Penn MS. 2008. Permeability change of arterial endothelium is an age-dependent function of lesion size in apolipoprotein E-null mice. Am J Physiol Heart Circ Physiol 295:H2273–H2279.

McKenzie JA, Ridley AJ. 2007. Roles of Rho/ROCK and MLCK in TNF-alpha-induced changes in endothelial morphology and permeability. J Cell Physiol 213:221–228.

Miao H, Hu YL, Shiu YT, Yuan S, Zhao Y, Kaunas R, Wang Y, Jin G, Usami S, Chien S. 2005. Effects of flow patterns on the localization and expression of VE-cadherin at vascular endothelial cell junctions: In vivo and in vitro investigations. J Vasc Res 42:77–89.

Miyazaki T, Ise M, Seo H, Niwa T. 1997. Indoxyl sulfate increases the gene expressions of TGF-beta 1, TIMP-1 and pro-alpha 1(I) collagen in uremic rat kidneys. Kidney Int Suppl 62:S15–S22.

Motojima M, Hosokawa A, Yamato H, Muraki T, Yoshioka T. 2003. Uremic toxins of organic anions up-regulate PAI-1 expression by induction of NF-kappaB and free radical in proximal tubular cells. Kidney Int 63:1671–1680.

Nielsen LB, Nordestgaard BG, Stender S, Kjeldsen K. 1992. Aortic permeability to LDL as a predictor of aortic cholesterol accumulation in cholesterol-fed rabbits. Arterioscler Thromb 12:1402–1409.

Niwa T, Ise M. 1994. Indoxyl sulfate, a circulating uremic toxin, stimulates the progression of glomerular sclerosis. J Lab Clin Med 124:96–104.

Niwa T, Takeda N, Tatematsu A, Maeda K. 1988. Accumulation of indoxyl sulfate, an inhibitor of drug-binding, in uremic serum as demonstrated by internal-surface reversed-phase liquid chromatography. Clin Chem 34:2264–2267.

Ogunrinade O, Kameya GT, Truskey GA. 2002. Effect of fluid shear stress on the permeability of the arterial endothelium. Ann Biomed Eng 30:430–446.

Owada S, Goto S, Bannai K, Hayashi H, Nishijima F, Niwa T. 2008. Indoxyl sulfate reduces superoxide scavenging activity in the kidneys of normal and uremic rats. Am J Nephrol 28:446–454.

Rackow EC, Fein IA, Sprung C, Grodman RS. 1978. Uremic pulmonary edema. Am J Med 64:1084–1088.

Rocha M, Apostolova N, Hernandez-Mijares A, Herance R, Victor VM. 2010. Oxidative stress and endothelial dysfunction in cardiovascular disease: Mitochondria-targeted therapeutics. Curr Med Chem 17:3827–3841.

Sanchez T, Skoura A, Wu MT, Casserly B, Harrington EO, Hla T. 2007. Induction of vascular permeability by the sphingosine-1-phosphate receptor-2 (S1P2R) and its downstream effectors ROCK and PTEN. Arterioscler Thromb Vasc Biol 27:1312–1318.

Schwenke DC, Carew TE. 1989. Initiation of atherosclerotic lesions in cholesterol-fed rabbits. I. Focal increases in arterial LDL concentration precede development of fatty streak lesions. Arteriosclerosis 9:895–907.

Shi S, Garcia JG, Roy S, Parinandi NL, Natarajan V. 2000. Involvement of c-Src in diperoxovanadate-induced endothelial cell barrier dysfunction. Am J Physiol Lung Cell Mol Physiol 279:L441–L451.

Siflinger-Birnboim A, Goligorsky MS, Del Vecchio PJ, Malik AB. 1992. Activation of protein kinase C pathway contributes to hydrogen peroxide-induced increase in endothelial permeability. Lab Invest 67:24–30.

Sluimer JC, Kolodgie FD, Bijnens AP, Maxfield K, Pacheco E, Kutys B, Duimel H, Frederik PM, van Hinsbergh VW, Virmani R, Daemen MJ. 2009. Thin-walled microvessels in human coronary atherosclerotic plaques show incomplete endothelial junctions relevance of compromised structural integrity for intraplaque microvascular leakage. J Am Coll Cardiol 53:1517–1527.

Somlyo AP, Somlyo AV. 2003. Ca^{2+} sensitivity of smooth muscle and nonmuscle myosin II: Modulated by G proteins, kinases, and myosin phosphatase. Physiol Rev 83:1325–1358.

Taki K, Tsuruta Y, Niwa T. 2007. Indoxyl sulfate and atherosclerotic risk factors in hemodialysis patients. Am J Nephrol 27:30–35.

Tumur Z, Niwa T. 2009. Indoxyl sulfate inhibits nitric oxide production and cell viability by inducing oxidative stress in vascular endothelial cells. Am J Nephrol 29:551–557.

Usatyuk PV, Vepa S, Watkins T, He D, Parinandi NL, Natarajan V. 2003. Redox regulation of reactive oxygen species-induced p38 MAP kinase activation and barrier dysfunction in lung microvascular endothelial cells. Antioxid Redox Signal 5:723–730.

Vanholder R, De Smet R, Glorieux G, Argiles A, Baurmeister U, Brunet P, Clark W, Cohen G, De Deyn PP, Deppisch R, Descamps-Latscha B, Henle T, Jorres A, Lemke HD, Massy ZA, Passlick-Deetjen J, Rodriguez M, Stegmayr B, Stenvinkel P, Tetta C, Wanner C, Zidek W. 2003. Review on uremic toxins: Classification, concentration, and interindividual variability. Kidney Int 63:1934–1943.

Vanholder R, Massy Z, Argiles A, Spasovski G, Verbeke F, Lameire N. 2005. Chronic kidney disease as cause of cardiovascular morbidity and mortality. Nephrol Dial Transplant 20:1048–1056.

Wysolmerski RB, Lagunoff D. 1990. Involvement of myosin light-chain kinase in endothelial cell retraction. Proc Natl Acad Sci USA 87: 16–20.

Yamamoto H, Tsuruoka S, Ioka T, Ando H, Ito C, Akimoto T, Fujimura A, Asano Y, Kusano E. 2006. Indoxyl sulfate stimulates proliferation of rat vascular smooth muscle cells. Kidney Int 69:1780–1785.

Zhou X, Wen K, Yuan D, Ai L, He P. 2009. Calcium influx-dependent differential actions of superoxide and hydrogen peroxide on microvessel permeability. Am J Physiol Heart Circ Physiol 296:H1096–H1107.